Electronic Supplementary Material (ESI) for Nanoscale.
This journal is © The Royal Society of Chemistry 2023

Supplementary Information for

Nanoscale structural response of biomimetic cell membranes to controlled dehydration.

Emilia Krok[a*], Henri G. Franquelim[b,c], Madhurima Chattopadhyay[a], Hanna Orlikowska-Rzeznik[a], Petra Schwille[b], Lukasz Piatkowski[a*]

[a] Poznan University of Technology, Faculty of Materials Engineering and Technical Physics, Institute of Physics, Piotrowo 3, 60-965 Poznan, Poland
[b] Department of Cellular and Molecular Biophysics, Max Planck Institute of Biochemistry, Am Klopferspitz 18, 82152 Martinsried, Germany
[c] Leipzig University, Research and Transfer Center for Bioactive Matter, Deutscher Platz 5, 04103 Leipzig, Germany

*corresponding authors

Table of contents:

Supplementary note 1

To verify whether there are any changes in the detected fluorescence intensity of the Atto 633 dye due to other effects independent of the spatial rearrangement of the probe (partitioning), we acquired additional, control data and quantified the changes in the fluorescence intensity as a function of membrane hydration for a single-component, non-phase-separated SLB composed of 14:1 PC doped with DOPE-Atto 633 (0.1 mol%). Figure S3a shows that the detected fluorescence signal increases by a factor of approximately 1.6 with dehydration. Given the very high fluorescence quantum yield (QE) of Atto 633 (64% in water), it is not physically possible that the observed increase is solely due to the increase in QE of the dye, as this would indicate that the QE increases to a value >100%. We could not identify any theoretical or experimental work that would provide explicit information on the possible changes in QE of Atto 663 when dissolved in water and embedded in an SLB. However, recent experimental results have shown that the QE of Atto 647N and Atto 655 increases by 25% and 48% respectively when embedded in an SLB compared to when dissolved in water[1]. Similarly, extensive studies by Frantzeskos have shown that the QE of the basic Atto 633 chromophore - CP 149 - does not change by more than 30% when dissolved in solvents of different polarity[2].

The optical properties of the studied system also change as a function of hydration. For example, the efficiency of fluorescence collection is influenced (among other things) by the refractive index of the medium in which the emitting dipoles are located[3]. In bulk water, the fluorescence is emitted more symmetrically with respect to the substrate plane, whereas in dehydrated conditions (higher refractive index mismatch between the membrane (~1.47[4,5]) and air), the fluorescence is mostly emitted towards the substrate. Thus, the observed increase in fluorescence intensity most likely includes a contribution from the optical effects.

Irrespective of the exact contributions of the effects discussed above, we clearly observed (Fig. S3b) that the fluorescence signal of Atto 633 increases much less in the L_d phase (~x1.5) than in the L_o phase (~x4.7). Indeed, if redistribution of DOPE-Atto 633 were the only mechanism, one should observe an increase in fluorescence intensity in the L_o domain and a decrease (by the same absolute amount) of the fluorescence intensity in the adjacent L_d phase region. If we correct the observed increase in fluorescence intensity in the L_o/L_d phases by a factor of 1.6, determined from the single-component membrane, we find (Fig. S3c) that indeed the fluorescence intensity in the L_o phase increases (~600 counts), while in the L_d phase we observe a decrease in fluorescence intensity (~600 counts). Of course, any quantitative conclusions should be made with great caution, as not all the effects involved here are easily identifiable and quantifiable, but the acquired fluorescence data give a very solid indication of the increased mixing of lipids associated with the two phases.

Supplementary note 2

In the interphase height mismatch data shown in Figure 5a, we observed a sudden increase in the L_d-L_o height mismatch for the membrane in humid air (90% RH) compared to the membrane in water (100% RH). We consider this to be an artifact due to abrupt changes in the balance of attractive and repulsive forces to which the AFM tip is subjected immediately after the removal of bulk water. As mentioned in the main text, it was experimentally very difficult to obtain AFM images immediately after removal of bulk water. These samples were extremely sticky and the AFM tip dragged considerably, requiring multiple scans to first remove the membrane aggregates. This additional stickiness was mainly observed in AFM images taken during the dehydration trajectory (immediately after bulk water removal), as opposed to the rehydration trace (from dry to humid air). This is probably due to the presence of strong capillary and adhesive forces between the tip and sample during the dehydration phase, likely caused by the residual water molecules adsorbed on the silicon tip and the formation of a nanoscopic water meniscus[6,7]. These stronger tip-sample adhesion forces can lead to membrane deformation/compression[8], especially of the softer L_d regions, and consequently to an "overestimation" of the recorded L_d-L_o height difference values.

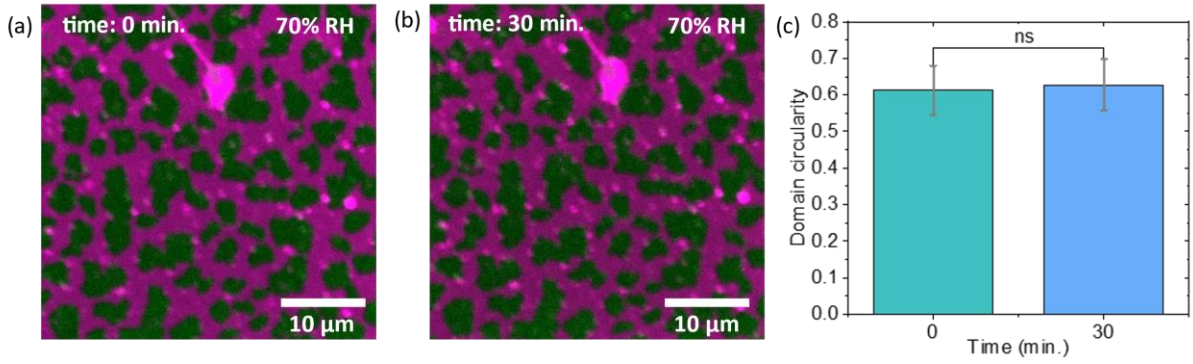

Fig. S1 Domains circularity measured as a function of time.
Fluorescence images of a representative SLB showing phase separation into L_d (labelled with DOPE-Atto 633, shown in magenta) and L_o (labelled with CTxB-Alexa 488, shown in green): (a) measured after equilibration with 70% RH and (b) after 30 min. incubation at 70% RH. (c) Domain circularity determined from the domains shown in (a) and (b).

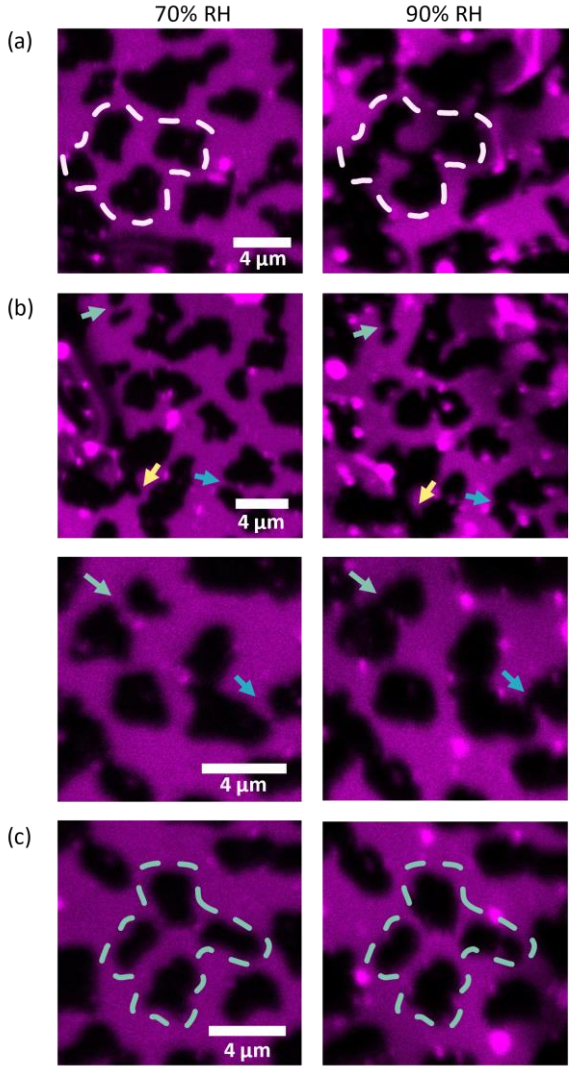

Fig. S2 Changes of the domains shape during rehydration
(a) Merging of domains as relative humidity is increased from 70 to 90% RH. The blue dashed lines mark the outlines of four merging domains. (b) Merging of domains during humidity increase, arrows indicate the merging points of the domains at 70 (left) and 90% RH (right). (c) Domains that did not merge during the increase of the environment relative humidity. Confocal imaging was performed in 10 mM HEPES and 150 mM NaCl buffer.

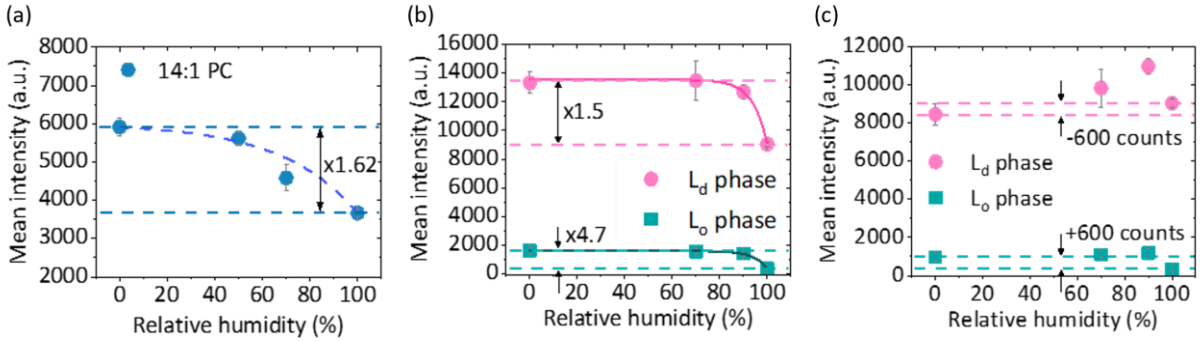

Fig. S3 Fluorescence signal from DOPE-Atto 633 probe as a function of membrane hydration
(a) Changes in the fluorescence intensity of the L_d phase probe - DOPE-Atto 633 during the dehydration cycle of a single component SLB composed of 14:1 PC. (b) Changes in the fluorescence intensity of the DOPE-Atto 633 probe measured separately in the L_d and L_o phases during dehydration of a phase-separated SLB. (c) Corrected changes in the fluorescence intensity of the DOPE-Atto 633 probe during dehydration. The correction factor of 1.62 was calculated from the changes in fluorescence intensity observed for a single component membrane.

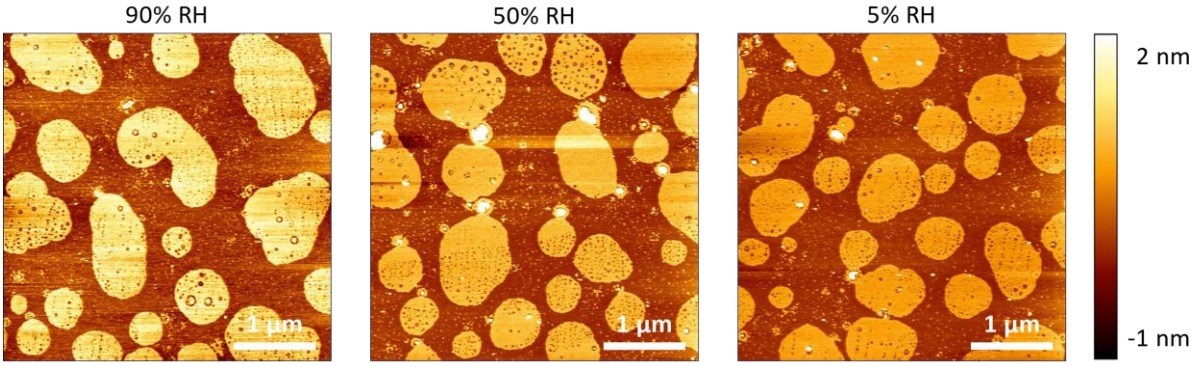

Fig. S4 AFM topography images of SLBs during dehydration
Representative images of SLBs during the dehydration cycle. The membrane was equilibrated at 90, 50 and 5% RH.

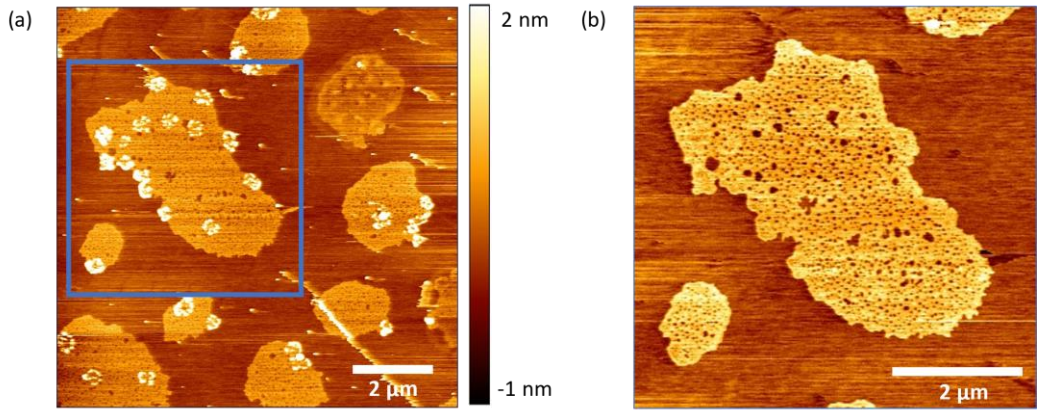

Fig. S5 AFM topography images of SLBs right after removal of bulk water
(a) Representative image of the lipid bilayer immediately after removal of bulk water and equilibration to 90% RH. The blue square indicates the area shown in high resolution images of the lipid bilayer at 90% RH (b). The lipid membrane was sticky at high humidity, small aggregates on the surface were dragged by the tip, causing distortions in the measurements. (b) After further equilibration and sweeping with the AFM tip over the surface, the aggregates on top of the membrane were removed and the topography could be measured more reliably.

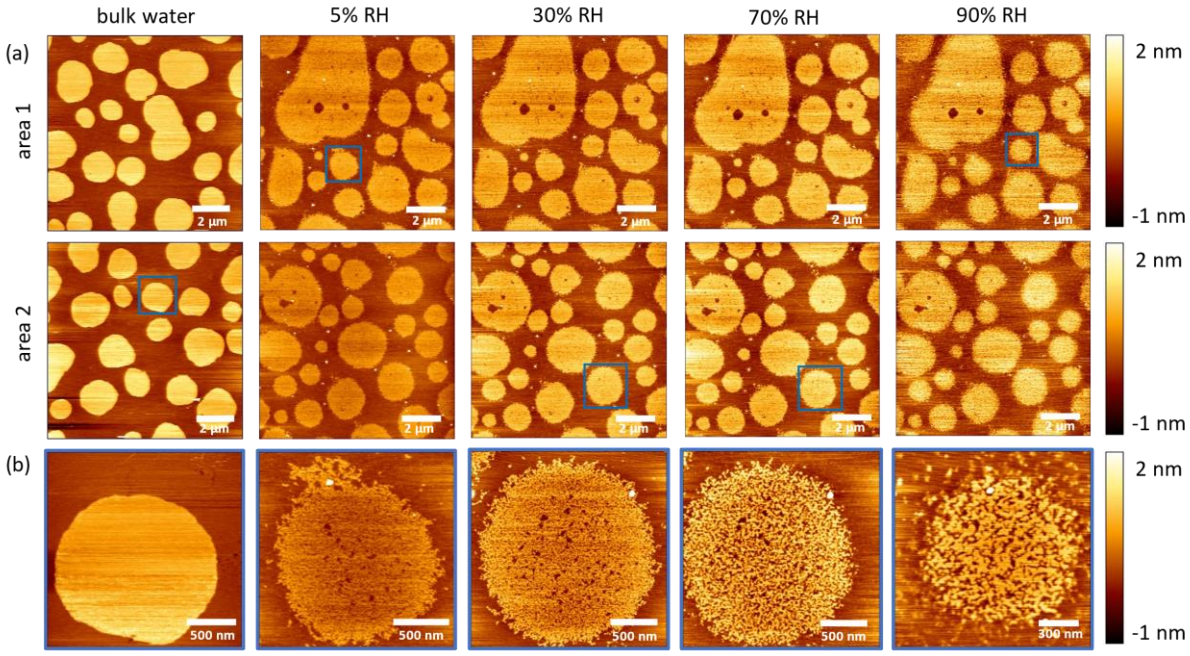

Fig. S6 AFM topography images of SLBs at different hydration levels.
(a) Representative images of fully hydrated SLB, and SLB after removal of bulk water and equilibration at 5, 30, 70 and 90% RH. The top and middle rows correspond to two different regions of the SLB. (b) High resolution images of individual areas (indicated by blue squares in panel (a)) at different hydration levels.

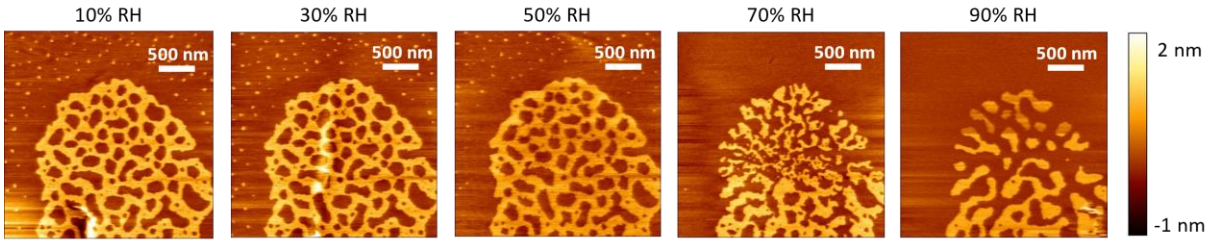

Fig. S7 High resolution AFM topography images of single L_o phase domain at different hydration levels. High resolution single domain images during membrane rehydration revealed the evolution of the L_d nanodomains trapped within the L_o phase. At 70% RH, it is evident that the L_d phase nanodomains merge to minimize the phase boundary.

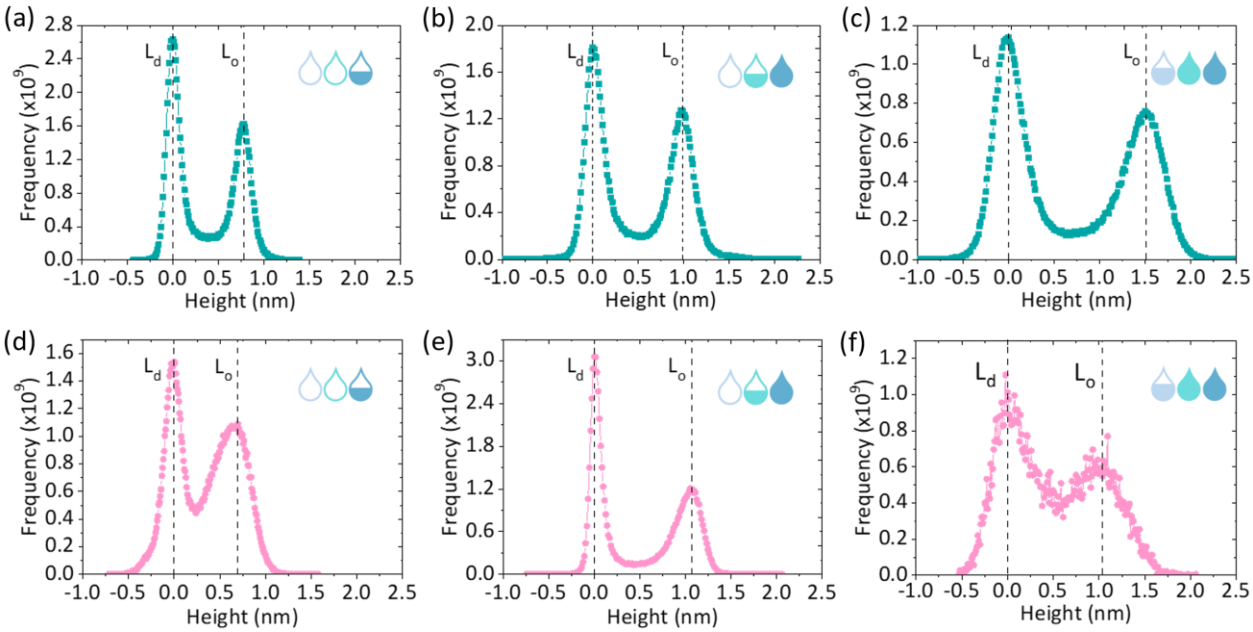

Fig. S8 Quantification of the height difference between the L_d and L_o phase from the AFM images. Height distribution histograms for the membrane subjected to dehydration (top row, green) at (a) 5% RH, (b) 50% RH, and (c) 90% RH, and rehydration (bottom row, pink) at (d) 5% RH, (e) 50% RH, and (f) 90% RH. The profiles have been offset corrected so that the L_d peak is centered at 0 nm.

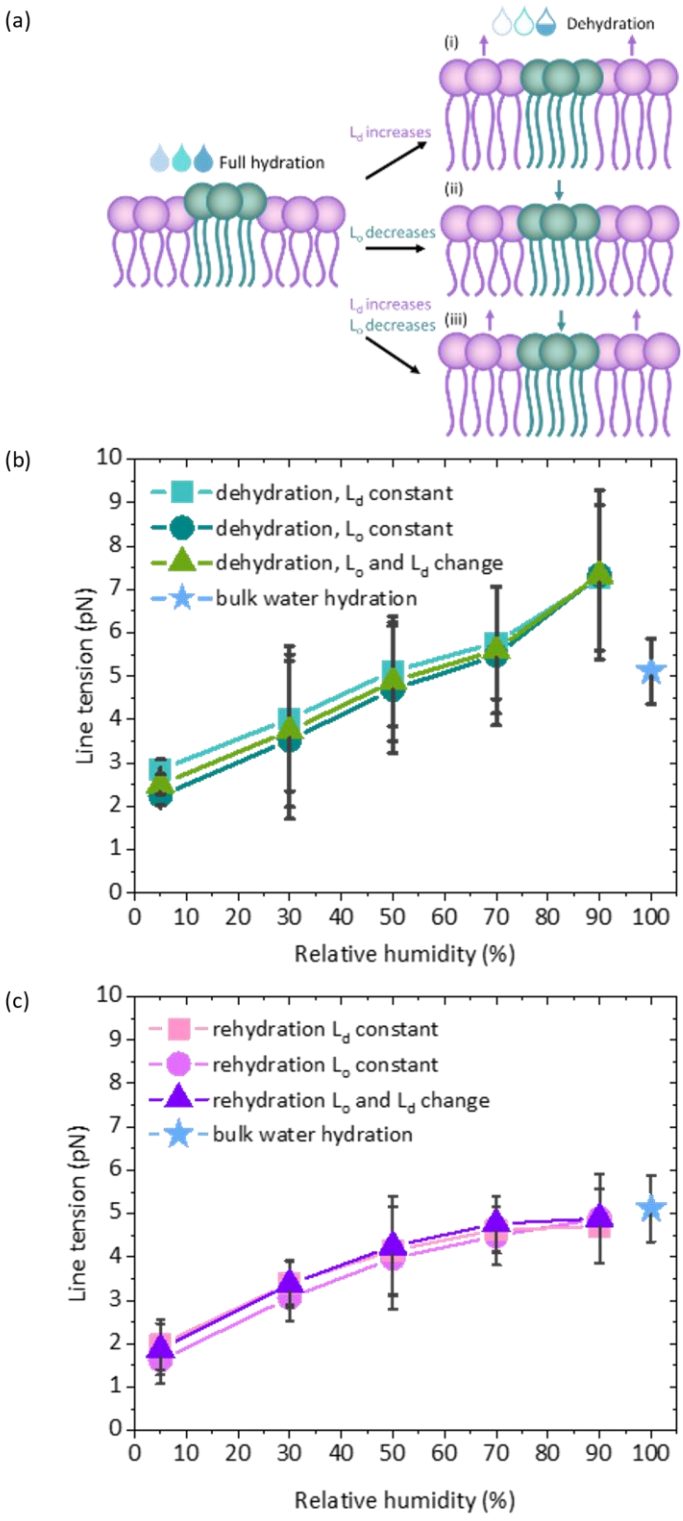

Fig. S9 Line tension at different hydration levels during dehydration and rehydration of the lipid bilayer. (a) Three scenarios for the line tension calculation: (i) the L_d phase thickness increases, while the L_o phase does not change, (ii) the L_o phase thickness decreases, while the L_d phase thickness does not change, (iii) the L_d phase increases and the L_o phase decreases. (b) Line tension during dehydration calculated from the model assuming a soft domain and no spontaneous curvature for the three different scenarios shown in (a). (c) Line tension during rehydration calculated for the three different scenarios presented in (a).

References:

1 F. Schneider, D. Ruhlandt, I. Gregor, J. Rg Enderlein and A. I. Chizhik, Quantum Yield Measurements of Fluorophores in Lipid Bilayers Using a Plasmonic Nanocavity, *J. Phys. Chem. Lett*, 2017, **8**, 1472–1475.

2 Jörg Frantzeskos, *Neue langwellige Fluoreszenzfarbstoffe zur Markierung von Biomolekülen*, Shaker Publishing House, 2001.

3 D. Axelrod, in *Fluorescence Microscopy: Super-Resolution and other Novel Techniques*, Academic Press, 2014, pp. 1–14.

4 D. F. Kienle, J. V. De Souza, E. B. Watkins and T. L. Kuhl, Thickness and refractive index of DPPC and DPPE monolayers by multiple-beam interferometry, *Anal. Bioanal. Chem.*, 2014, **406**, 4725–4733.

5 A. Gadomski, N. Kruszewska and J. M. Rubi, Derivation of the refractive index of lipid monolayers at an air-water interface, *Opt. Mater.*, 2019, **93**, 1–5.

6 X. Xiao and L. Qian, Investigation of humidity-dependent capillary force, *Langmuir*, 2000, **16**, 8153–8158.

7 D. I. Kim, J. Grobelny, N. Pradeep and R. F. Cook, Origin of adhesion in humid air, *Langmuir*, 2008, **24**, 1873–1877.

8 A. San Paulo and R. García, High-Resolution Imaging of Antibodies by Tapping-Mode Atomic Force Microscopy: Attractive and Repulsive Tip-Sample Interaction Regimes, *Biophys. J.*, 2000, **78**, 1599–1605.